POLITECNICO DI TORINO
Repository ISTITUZIONALE

Low-cost and environmentally friendly physic-mechanical pre-treatments to recycle lithium iron phosphate cathodes

(Article begins on next page)

11 February 2024

Low-cost and environmentally friendly physic-mechanical pre-treatments to recycle lithium iron phosphate cathodes

Martina Bruno , Silvia Fiore *

DIATI, Department of Environment, Land and Infrastructure Engineering, Politecnico di Torino – Corso Duca degli Abruzzi, 24, 10129 Torino, Italy

ARTICLE INFO

ABSTRACT

Recycling Lithium Iron Phosphate (LFP) batteries is challenging, as their low economic value hinders the profitability of full-scale processes. Optimized pre-treatments are crucial for the overall efficiency and economic profitability of recycling processes. This study explored chemicals-free physic-mechanical pre-treatment processes aimed to detach waste LFP cathodes (production scraps and end-of-life, EoL) from aluminium current collectors. The technical performances of ultrasounds (35 kHz, in water at 25 °C for 5, 15, 30 min), ball milling (840–1080 rpm for 8, 16, 24 min), and thermal treatment (30 min at 200, 250, 300, 350,°C) coupled with ball milling (840 rpm for 5 min) have been compared. Environmental impacts and economic cost were calculated based on energy demand. The highest separation efficiency achieved were $95 \pm 5\%$ for Li, $99 \pm 6\%$ for Fe, and $80 \pm 3\%$ for P in scrap cathodes, treated at 200 °C for 30 min and ball milled at 840 rpm for 5 min; $93 \pm 15\%$ for Li, $97 \pm 21\%$ for Fe and $82 \pm 20\%$ for P in EoL cathodes, treated at 250 °C for 30 min and ball milled. The global warming impacts were: 3.33 ± 0.55 kg CO_2 eq/kg of detached cathode for scraps and 3.08 ± 0.25 kg CO_2 eq/kg for EoL cathodes; the costs were 1.45 ± 0.24 €/kg of detached cathode for production scraps samples and 1.34 ± 0.11 €/kg for EOL samples. In conclusion, chemicals-free mechanical detachment was effective both for production scraps and EoL cathodes, while thermal treatment was especially beneficial for EoL cathodes, and reducing milling time improved the environmental impacts and costs of the pre-treatment processes.

1. Introduction

Lithium-ion batteries' (LIBs) market is expected to reach 2000 GWh by 2030 [1], mainly due to electrification of transport systems [2], and recycling waste batteries is crucial to meet the forecasted raw materials' demand [3,4]. From an environmental point of view, recycling holds a significant role in limiting the impacts of LIBs' life cycle [5] by avoiding unproper end of life (EOL) management [6] and saving energy and environmental impacts associated with primary materials' mining [7]. LIBs can enclose different types of cathodes; the most common (29% of market in 2020) are nickel manganese cobalt (NMC) cathodes [1], while market for lithium iron phosphate (LFP) chemistry is expected to grow globally from 0.4 billion USD in 2017 to 15.24 UDS by 2027 [2]. LFP are forecasted to consistently represent the second most common battery chemistry, after NMC, in the global production capacity until 2030 [2]. LFP batteries ensure fast charging rates, long life span and high stability [3,4]. The absence of cobalt, nickel and manganese in LFP batteries limits the costs associated with their production [5].

Full-scale LIBs' recycling is based on pyrometallurgy and hydrometallurgy technologies [8], whose economic profitability is guaranteed by the recovery of valuable metals (cobalt, nickel, manganese, copper, aluminium) enclosed in cathodes and current collectors [9]. The economic sustainability of recycling LFP batteries is challenging because of the limited market value of the raw materials [10]. LIBs' recycling technologies are deeply affected by physic-mechanical pre--treatments [11] and the overall recycling efficiency and economic viability may be compromised by material loss during pre-treatments [12,13]. The liberation of electrode active materials from current collector, binder and electrolyte has been highlighted as key phase [14]. Recent studies on LFP batteries' recycling mostly investigated hydrometallurgy processes based on inorganic acids, as sulfuric acid [15–18] and hydrochloric acid [19] and on organic acids [20]. Literature specifically involving pre-treatments applied to LFP cathodes is limited [21].

The scientific community has already explored the liberation of electrode materials in LCO and NMC batteries via mechanical (ultrasounds and ball milling), chemical, thermal processes, and their combinations [6,8,12] to remove binder and electrolyte and detach the

---

active materials from current collectors. Binders' removal was studied by applying organic solvents [22] or thermal processes at 400–450 °C for up to 2 h [23–25], or at 500–550 °C for shorter times [26–28]. Ultrasounds have been tested to mechanically detach the active materials at 20–45 kHz [29–31], mostly at room temperature [29,31–33] for up to 2 h [31,34], also in combination with sulfuric [35,36], citric [37,38] and DL-malic [39,40] acids. Besides, a remarkable amount of energy gets dissipated as heat, limiting comminution capacity at standard rates met by shredding [41]. Pre-treatments based on ball milling [42] and other purely mechanical processes [43–46] have been explored, also in combination with acids in mechano-chemical processes [28,47,48], significantly increasing metals' recovery by increasing the specific surface area of the detached materials [49] and limiting energy requirements [50].

Based on the analysis of the above-mentioned literature, the operational parameters (power consumption, frequency, temperature, and time) have been summarized and compared (Appendix Figure A1). It should be noticed that each detachment method has different operative conditions. As expected, thermal treatment requires higher temperature compared to ultrasound washing and ball milling. Lower temperatures demand longer treatment times: below 500 °C, the duration of thermal treatment varies between 1.5 [25] and 2 h [23,24]. When not combined with acid leaching, ultrasound washing usually happens at room temperature [30–33], whereas mechanochemical ultrasound washing requires temperatures ranging between 40 °C [51] and 80 °C [39]. Ball milling, on the other hand, is usually performed at room temperature [13,52] and requires less time than ultrasound washing and thermal treatment.

Ultrasounds' efficiency in liberation was equal to 46% separation and 15% aluminium foil purity [36] in water, and improved to 99% when sulfuric or oxalic acid [36], hydrogen peroxide [34] or N-Methyl-2-Pyrrolidone (NMP) were used [41]. Mechanical detachment via ball milling achieved excellent cathode material recovery rates of 99% when followed by Eddy current separation [51,53], 92% to 97% when followed by pneumatic separation [54,55] and 95% when followed by sieving [56]. When pyrolysis was applied as thermal treatment, recovery rates ranged from 80% [52] to 85% [57]. Incineration increased efficiency of mechanical crushing, achieving recovery rates between 89% [58] and 93% [53].

However, despite physical methods for detachment of cathode material from current collectors are highly efficient, they add to the cost of battery recycling. To the best of our knowledge, only a few studies investigated mechanical detachment for cathode materials with low economic value, such as LFP, instead of focusing on other cathodes such as LCO [59,60] or NMC [33,61]. Moreover, previous studies assessed specific technologies, such as ultrasound washing [29–34], ball milling [13,24,42,59] and thermal treatments [23–28], and they considered only end-of-life cathodes [18–21,31,32–42,53,54–57], completely ignoring production scraps. Additionally, earlier research focused on the technical performances of detachment methods, such as separation efficiency and material grade, but energy consumption and environmental impacts were overlooked.

Compared to existing literature, this work is centred on mechanical detachment of cathodic materials from LFP cathodes, comparing three processes (ultrasound washing, thermal treatment and ball milling, also combined), without application of chemical reagents. Among the options reported by state-of-the-art literature, the choice of the explored pre-treatments was based on performances and on ease of application and absence of chemicals. Two samples of LFP cathodes have been studied: production scraps (PS) and end of life cathodes (EOL). Ultrasound washing, thermal treatment and ball milling have been optimized by varying intensity, temperature, and duration. Energy consumption during the application of the detachment methods was measured to compare the associated costs and environmental impacts.

2. Materials and methods

2.1. Materials and equipment

The samples were waste LFP cathodes of two types: production scraps (defined PS in the following) and end-of-life cathodes (defined EOL in the following). Before pre-treatment tests, the samples have been manually cut in 0.5 cm pieces.

The pre-treatment tests were studied at lab scale through the following equipment (Appendix Figure A2): a Retsch MM200 ball mill (50 mL milling jars with two 10 mm-beads in zirconium oxide in each jar); a ZE muffle furnace (maximum temperature 1100 °C); a Bandelin SONOREX DIGIPLUS DL 514 BH ultrasonic bath (ultrasonic peak power 720 W, ultrasonic nominal power 180 W, ultrasound frequency 35 kHz, power settings between 20%−100% and temperature range 20–80 °C); an ARGO LAB TCN 30 oven (maximum temperature 200 °C). The energy requirements of the pre-treatments were measured through a Maxcio PM10 power meter.

The samples have been manually scraped with a spatula to detach the active materials from the current collector prior characterization. Material losses (i.e., fine particles) due to manual scraping accounted for 9%wt. for PS and 4%wt. for EOL. The products of the pre-treatments were manually sieved to separate the fraction having dimensions below 1 mm. The samples and the products of the pre-treatments were characterized through a GFA-EX7 Schimadzu Flame Atomic Absorption (FAA) Spectrometer to analyze lithium, and a Rigaku NEX-DE X-ray fluorescence (XRF) spectrometer to analyze aluminium, iron and phosphorous. The samples characterized with FAA spectrometry were pre-digested in a MILESTONE ETHOS UP microwave system: 500 mg of each sample were treated in 50 mL of 0.2 M HNO_3 and 0.8 M HCl at 230 °C for 25 min. Eventually, information about superficial morphology and granulometry of the initial samples and the detached active material were acquired using Phenom XL scanning electron microscopy and energy dispersive spectrometer (SEM-EDS). An acceleration voltage of 15 keV and a secondary electron detector were used.

2.2. Pre-treatments

The experimental design of this study (Fig. 1) involved three pre-treatment processes: ultrasounds washing, ball milling and thermal treatment followed by ball milling.

The optimization of operative parameters started from existing literature (Fig. 1). Ultrasounds washing was tested at room temperature (25 °C), applying 35 kHz for 5, 15 and 30 min. Ball milling was tested at 1080 rpm for 8, 16 and 24 min, and at 840 rpm for 16 min. Thermal treatment was tested at 200, 250, 300 and 350 °C for 30 min in air atmosphere and followed by ball milling at 840 rpm for 5 min. The samples were fed to the muffle furnace at room temperature, then the temperature was increased with a rate of 10 °C/min and kept constant for 30 min. Afterwards the samples were left in the furnace cooling down and remove from it when room temperature was reached. The thermal treatment temperature was kept below 350 °C to minimize oxidation of the Fe contained in the cathode materials [62]. Each test in the above-specified conditions was performed on 1.5 g of sample and in 3 replicates. The specific energy demand was calculated by measuring the electricity consumption through a Maxcio power meter. Energy demand measurements have been adjusted to account for the maximum capacity of the equipment.

The comparison of pre-treatments was based on Key Performance Indicators (KPIs): recovery rate of Li, Fe and P in cathode powder (%), %-wt. impurities in cathodes powders after pre-treatments, material loss (%-wt.) and specific energy demand (kWh/kg). The recovery rate (η_x) was calculated based on the mass balance of Li, Fe and P, where $m_p(x)$ is the mass of Li, Fe and P in the cathode powder after physical detachment, and $m_0(x)$ is the mass of Li, Fe and P in the initial samples (Eq. 1).
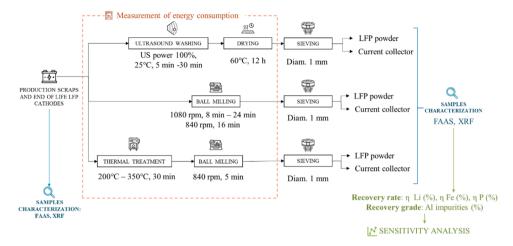
Fig. 1. Experimental design of the mechanical detachment of LFP cathodes (production scraps PS, and end-of-life EOL) from aluminium current collectors (FAAS: flame atomic absorption spectrometry, LFP: Lithium Iron Phosphate, US: ultrasound, XRF: X-ray fluorescence spectrometry).

$$\eta_x = \frac{m_p(x)}{m_0(x)} \tag{1}$$

2.3. Sensitivity analysis

The experimental results were statistically analysed to identify potential correlations by applying Pearson's bivariate correlation tests on Excel (Microsoft Office).

2.4. Environmental and economic assessments

The environmental and economic assessments were based on the obtained experimental results; they should be considered purely preliminary and aimed at comparing the pre-treatments. To allow comparison among pre-treatments, based on various equipment at lab scale, all experimental results were scaled up referring to a functional unit equal to 1 kg of LFP cathodes processed. Besides, the scale-up of the consumption of energy and water considered the processing capacity of the equipment applied, which amounts to 1.8 kg of samples (corresponding to 18 l of water) for the ultrasound bath, 50 g of samples for the muffle furnace and 5 g for the ball mill. The environmental impacts of the tested pre-treatments have been calculated according to impact method Recipe 2016 v1.03 midpoint (H) (Appendix Table A1) and coefficients retrieved from Ecoinvent 3.9.1 database [63]. The economic analysis was based on the specific energy demand (Section 2.2), on the use of deionised water, and on the operative costs detailed in the following: 0.1604 €/kWh, corresponding to average European price for energy consumption for non-households consumers [64], and $8.081 \cdot 10^{-5}$ €/kg for water cost in Europe [63]. The costs of the pre-treatment processes have been compared with 20.041 €/kg, which is the current market value for lithium iron phosphate powders according to Ecoinvent 3.9 database [63].

3. Results and discussion

3.1. Samples' characterisation

Manual scraping led to material losses; 12 ± 3%-wt. for EOL samples and 10 ± 0.8%-wt. for PS samples. These were respectively decreased to 4 ± 0.5%-wt. and 9 ± 2%-wt. when scraping happened in water. PS samples were made of 16%wt. current collectors and 80%wt. powders (including cathode active material and residual binder and electrolyte), while EOL of 13%wt. current collectors and 79% powders, in agreement with literature [65]. Aluminium content in metallic current collectors was 67.9 ± 15%wt. in PS and 79.7 ± 19%wt. in EOL, which is below

99.35%wt. of commercial current collectors [66]. The detached cathodic powders were made of lithium (2.1 ± 0.1%wt. in PS and 1.6 ± 0.001%wt. in EOL), iron (29.5 ± 4.5%wt in PS and 29.6 ± 1.3%wt in EOL), and phosphorous (16.4 ± 2.5%wt in PS and 14.8 ± 0.4%wt in EOL). These results are consistent with LFP cathodes active materials' composition (29.4 ± 5.2%wt iron, 15.9 ± 3.2%wt phosphorous and 4% wt lithium) reported by literature [65,67] (Appendix Figure A3).

3.2. Pre-treatments

The detachment treatments have been compared in terms of separation rate of Li, Fe and P (%), material loss (%) and Al impurities (%) in the cathode material for PS samples and EOL samples (Fig. 2). The separation efficiencies of PS and EOL samples differed for each detachment method, although comparable trends occurred. EOL samples achieved better separation efficiency than PS samples. Ultrasound washing was proved ineffective for the detachment of PS samples. Ball milling and thermal treatment followed by ball milling produced acceptable separation rates for both PS and EOL samples; however, the latter provided better results. Except during ultrasound washing, material loss was higher for PS samples. The loss of material caused by ultrasound washing of EOL samples was greater than the loss caused by manual scraping.

Ultrasounds washing was insufficient for the detachment of cathode materials from PS electrodes, leaving the samples almost unaltered (Fig. 3). Whereas EOL samples were detached via ultrasound washing with deionized water. However, separation rates of ultrasound washing were limited to 50 ± 6% for Li, 76 ± 14% for Fe and 69 ± 12% for P when the process was carried out for 30 min. The separation rate decreased when the process's duration was reduced: 41 ± 9% for Li, 55 ± 10% for Fe and 61 ± 11% for P after 15 min, and 30 ± 5% for Li, 32 ± 6% for Fe and 36 ± 7% for P after 5 min. Material loss was extensive during ultrasound washing; 66 ± 8% after 5 min, 53 ± 7% after 15 min and 46 ± 9% after 30 min. These results shouldn't be attributed to binder decomposition, since it is insoluble in water [34]. Whereas Al contamination in cathode material separated by ultrasound washing was minimal: 0.14 ± 0.02% after 5 min, 0.13 ± 0.01% after 15 min and 0.24 ± 0.01% after 30 min. The highest contamination of Al in the samples, as predicted, was associated with the longest duration of ultrasound washing.

Ultrasound washing did not significantly alter the superficial morphology of PS samples (Fig. 4A, 4B, 4C and 4D). The ultrasound force increased the dimension of existing cracks on the PS cathodes surface; however it did not separate the active material from the current collectors. Whereas plates of active material with dimensions over 1 mm
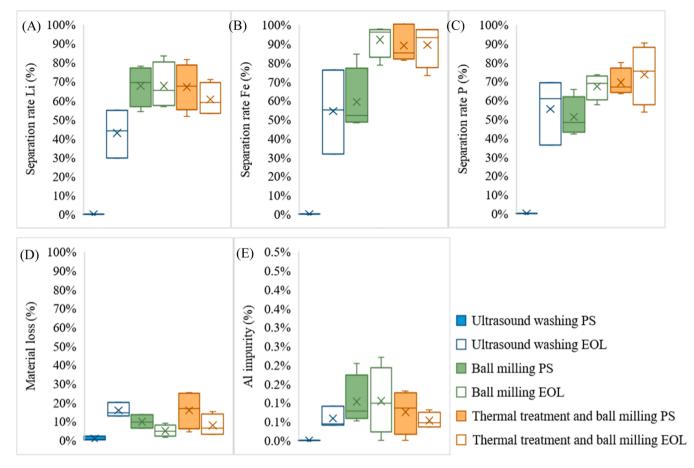
Fig. 2. Performances of the applied detachment treatments in terms of (A) Li separation rate (%), (B) Fe separation rate (%), (C) P separation rate (%), (D) material loss (%) and (E) Al impurities (%) for PS samples and EOL samples.
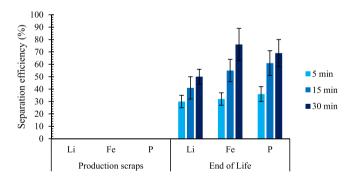

Fig. 3. Separation efficiency (%) for Li, Fe and P from current collectors after ultrasound washing.

were detached from EOL samples after ultrasound washing (Fig. 4F, 4G, 4H). Besides, the surface of the detached plates of active materials appears smoother than the surface of the initial EOL samples (Fig. 4E). Al concentration was below detection limits for SEM/EDS analyses.

Similarly to ultrasound washing, ball milling produced higher separation efficiencies for EOL samples rather than PS samples (Fig. 5). Separation rates for PS samples ball milled at 1080 rpm were as follows: $93 \pm 6\%$ for Li, $84 \pm 5\%$ for Fe and $66 \pm 5\%$ for P after 8 min, $74 \pm 8\%$ for Li, $48 \pm 11\%$ for Fe and $46 \pm 6\%$ for P after 16 min, $74 \pm 7\%$ for Li, $54 \pm 6\%$ for Fe and $50 \pm 5\%$ for P after 24 min. When the milling frequency was reduced to 840 rpm, separation rates of PS samples were not significantly altered: $68 \pm 2\%$ for Li, $50 \pm 4\%$ for Fe and $42 \pm 3\%$ for P. While separation rates for EOL samples ball milled at 1080 rpm were: $96 \pm 12\%$ for Li, $96 \pm 17\%$ for Fe and $67 \pm 16\%$ for P after 8 min, 99

$\pm 15\%$ for Li, $98 \pm 28\%$ for Fe and $70 \pm 16\%$ for P after 16 min, 74 $\pm 20\%$ for Li, $96 \pm 22\%$ for Fe and $73 \pm 14\%$ for P after 24 min. The following separation rate were obtained through ball milling of EOL samples at 840 rpm for 16 min: $97 \pm 13\%$ for Li, $79 \pm 18\%$ for Fe and $58 \pm 16\%$ for P. When the milling frequency of PS and EOL samples was raised, the separation rate increased. However, while separation rate appeared to be linearly influenced by milling time in EOL samples, this tendency did not emerge in PS samples. Besides, the duration of the milling process influences material losses during treatment: material loss was $16 \pm 4\%$ for PS samples and $17 \pm 6\%$ for EOL samples after 8 min at 1080 rpm, however it increases to $43 \pm 11\%$ for PS samples and $37 \pm 9\%$ for EOL after 24 min at the same frequency. Moreover, the longer the ball milling, the higher the Al concentration in the cathode powder after separation. Furthermore, different milling frequencies used for the same time (16 min) produced similar amounts of Al impurities: $0.27 \pm 0.74\%$ at 1080 rpm and $0.25 \pm 0.21\%$ at 840 rpm for PS samples, and $0.32 \pm 0.21\%$ at 1080 rpm and $0.28 \pm 0.29\%$ for EOL samples.

The granulometry of active material separated after ball milling differs depending on milling settings and between PS and EOL samples (Fig. 6). The grains of active material in EOL samples seem coarser than those in PS samples. Furthermore, the granulometry of detached active material after milling at 840 rpm is more homogeneous than in higher frequency milled samples.

Thermal treatments at temperatures below 350 °C generated no noticeable change in the samples, whether they were PS or EOL. However, a similar trend between process temperature and material loss has been found after thermal treatment (Appendix Figure A4). The difference in weight upon thermal treatment is directly proportional to the
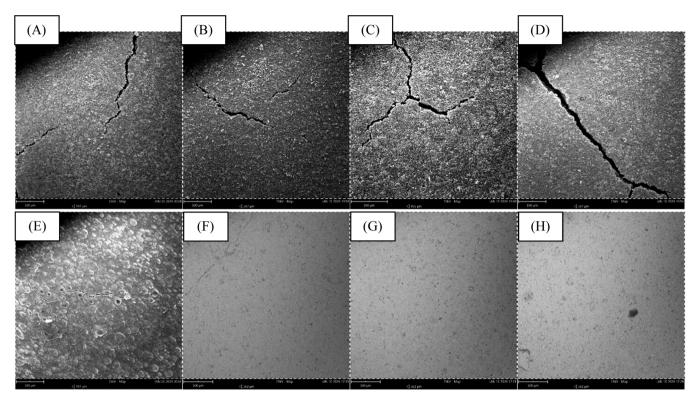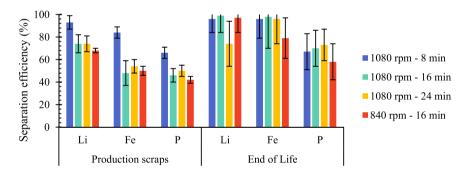
Fig. 4. SEM images of (A) PS initial sample and (B) after ultrasound washing for 5 min, (C) 15 min, (D) 30 min and (E) EOL initial sample and (F) after ultrasound washing for 5 min, (G) 15 min, (H) 30 min.

Fig. 5. Separation efficiency (%) for Li, Fe and P from current collectors after ball milling.

process temperature and it was greater in EOL samples than in PS samples. This observation is consistent with the beneficial effect of thermal treatment on the removal of residual electrolyte from EOL cathodes, as reported by previous studies [13,24]. After thermal treatment, PS and EOL samples have been ball milled at 840 rpm for 5 min (Fig. 7). Separation rates observed in PS samples were: $95 \pm 5\%$ for Li, $99 \pm 6\%$ for Fe and $80 \pm 3\%$ for P when temperature of the thermal treatment was 200 °C, $66 \pm 4\%$ for Li, $86 \pm 5\%$ for Fe and $67 \pm 6\%$ for P when temperature of the thermal treatment was 250 °C, $85 \pm 2\%$ for Li, $81 \pm 3\%$ for Fe and $63 \pm 3\%$ for P when temperature of the thermal treatment was 300 °C, and $91 \pm 7\%$ for Li, $83 \pm 8\%$ for Fe and $67 \pm 12\%$ for P when temperature of the thermal treatment was 350 °C. Separation rate of EOL samples instead were: $72 \pm 11\%$ for Li, $73 \pm 17\%$ for Fe and $54 \pm 10\%$ for P when temperature of the thermal treatment was 200 °C, $93 \pm 15\%$ for Li, $97 \pm 21\%$ for Fe and $82 \pm 20\%$ for P when temperature of the thermal treatment was 250 °C, $87 \pm 16\%$ for Li, $97 \pm 22\%$ for Fe and $90 \pm 21\%$ for P when temperature of the thermal treatment was 300 °C, and $67 \pm 11\%$ for Li, $89 \pm 16\%$ for Fe and $69 \pm 12\%$ for P when temperature of the thermal treatment was 350 °C. The temperature of the process had no effect on the material

losses observed during thermal treatment followed by ball milling. Similarly to separation efficiency, Al content declined in EOL samples heated at higher temperatures, from 0.13% in samples treated at 250 °C to 0.06% in those treated at 350 °C. The granulometry of milled active material after thermal treatment (Fig. 8) is coarser when temperature of the thermal treatment was below 250 °C, both for PS and EOL samples. However, active material detached from PS samples presents finer particles compared with EOL samples, regardless of temperature of the initial thermal treatment. The active material detached from EOL samples after thermal treatment at 200 °C and ball milling is the only sample that presented an Al concentration above the detection limit of SEM/EDS analyses, amounting to 0.51 at%.

Eventually, all detachments methods performed better for EOL samples. Thermal treatment followed by ball milling produced the best results for both PS and EOL samples. After thermal treatment at 200 °C followed by ball milling, the maximum separation rates for PS samples were: $95 \pm 5\%$ for Li, $99 \pm 6\%$ for Fe, and $80 \pm 3\%$ for P. While thermal treatment at 250 °C and ball milling of EOL samples corresponds to $93 \pm 15\%$ for Li, $97 \pm 21\%$ for Fe and $82 \pm 20\%$ for P, with material loss of 3% and aluminium content of 0.13%. Previous studies reported similar
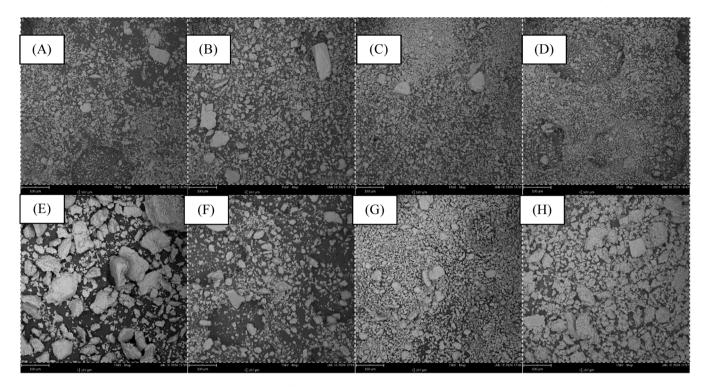
Fig. 6. SEM images of (A) active material from PS samples after milling at 1080 rpm for 8 min, (B) 16 min, (C) 24 min, and (D) at 840 rpm for 16 min; and (E) active material from EOL samples after milling at 1080 rpm for 8 min, (F) 16 min, (G) 24 min and (H) at 840 rpm for 16 min.
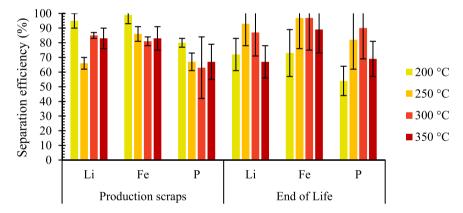

Fig. 7. Separation efficiency (%) for Li, Fe and P from current collectors after thermal treatment and ball milling.

separation efficiency: 90–97% of cathode material [26,27] with thermal treatment at higher temperature up to 500 °C.

3.3. Correlation analysis

A correlation analysis was carried out between the KPIs describing the performances of the pre-treatment processes and the operational parameters for PS and EOL samples, e.g., origin of the samples (PS or EOL), duration of ultrasound washing (5, 15 or 30 min), temperature of the muffle furnace (200 °C, 250 °C, 300 °C or 350 °C), frequency of ball milling (840 rpm or 1080 rpm) and duration of ball milling (5, 8, 16, 24 min) (Appendix, Table A5 e Table A6).

The correlation between separation efficiency of the cathode powder's main components was strong for PS samples ($r^2 =94\%$ between Li and Fe, $r^2 =97\%$ between Li and P and $r^2 =99\%$ between Fe and P) and EOL samples ($r^2 =84\%$ between Li and Fe, $r^2 =57\%$ between Li and P and $r^2 =85\%$ between Fe and P). Despite similar patterns can be observed for both PS and EOL samples, the key difference was in the

efficiency of ultrasound washing. Longer ultrasound washing times enhanced material loss in EOL samples ($r^2 =42\%$), however they didn't affect the purity of the separated material ($r^2 =-3\%$).

Temperature of thermal treatment had limited positive effect on cathode material separation efficiency, which was stronger for PS samples ($r^2 =50\%$ for Li, $r^2 =66\%$ for Fe and $r^2 =62\%$ for P) compared with EOL samples ($r^2 =17\%$ for Li, $r^2 =35\%$ for Fe and $r^2 =46\%$ for P).

The time and intensity of ball milling had the greatest influence on the detachment methods' performance. Higher milling frequency increased the separation of cathodes materials both for PS samples ($r^2 =94\%$ for Li, $r^2 =82\%$ for Fe and $r^2 =88\%$ for P) and EOL samples ($r^2 =88\%$ for Li, $r^2 =82\%$ for Fe and $r^2 =48\%$ for P). Longer duration of the milling process, instead, affected the content of Al impurities in the separated materials ($r^2 =86\%$ for PS samples and $r^2 =76\%$ for EOL samples) with a modest impact on the separation rate of the cathodes' main components ($r^2 =51\%$ for Li, $r^2 =26\%$ for Fe, $r^2 =36\%$ for P in PS samples and $r^2 =61\%$ for Li, $r^2 =54\%$ for Fe, $r^2 =23\%$ for P in EOL samples).
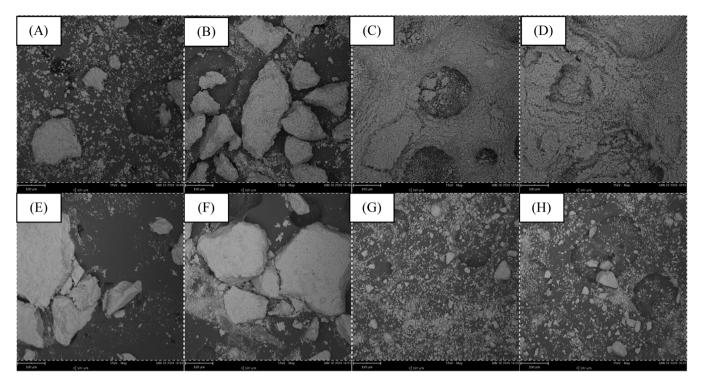
Fig. 8. SEM images of (A) active material from PS samples after milling at 1080 rpm for 8 min, (B) 16 min, (C) 24 min, and (D) at 840 rpm for 16 min; and (E) active material from EOL samples after milling at 1080 rpm for 8 min, (F) 16 min, (G) 24 min and (H) at 840 rpm for 16 min.

Another significant difference between PS and EOL samples was the correlation among material loss and separation rate of Li, Fe, and P. The physical connection between the cathode powder and the current collectors was stronger in PS samples because the binder had not yet been deteriorated. As a result, during mechanical detachment, part of the cathode powder stays attached to the current collectors, limiting the separation rate but not changing the material loss of the processes. Whereas, the main limit to separation efficiency for the EOL samples consisted in the loss of fine materials during the detachment: the higher the material loss, the lower the recovery rate ($r^2 = -89\%$ for Li, $r^2 = -90\%$ for Fe, $r^2 = -78\%$ for P).

3.4. Environmental and economic assessments

During the experimental activities, the energy and water consumptions were measured and scaled to 1 kg samples processed by each pre-treatment (Appendix Table A7). Energy consumption of the ultrasound bath (0.117 kWh for 5 min, 0.123 kWh for 15 min and 0.125 kWh for 30 min) and the muffle furnace (1.15 kWh for 30 min) employed during ultrasound washing and thermal treatment, were higher than those measured during ball milling (0.004 kWh for 5 min at 840 rpm, 0.009 kWh for 8 min at 1080 rpm, 0.016 for 16 min at 1080 rpm, 0.028 for 24 min at 1080 rpm and 0.013 for 16 min at 840 rpm). However, they allowed to process larger samples' amounts, reducing the specific energy requirement. Considering the treatment capacity of those equipment, the specific energy demand was 6.75 kWh/kg of input material for thermal treatment followed by ball milling; between 2.25 and 7.00 kWh/kg of input material for ball milling; and between 0.59 and 0.63 kWh/kg of input material for ultrasound washing. Then, to account for the different performance of alternative procedures, energy demands were calculated using the amount of detached cathode powder (Fig. 9).

Due to the poor performance of ultrasound washing on the detachment of PS samples, estimating its energy and water consumption to detach 1 kg of PS samples was not possible. EOL samples, on the other hand, required the least amount of energy to recover 1 kg of cathode material through ultrasound washing: 1.73 ± 0.2 kWh/kg of detached cathode material after 5 min, 1.30 ± 0.1 kWh/kg after 15 min and 1.16 ± 0.2 kWh/kg after 30 min. Because the separation rate of ultrasound
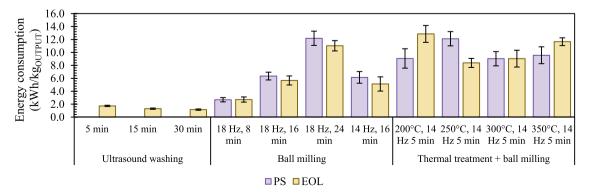

Fig. 9. Energy consumption (kWh/kg$_{OUTPUT}$) associated to the pre-treatment processes applied to lithium iron phosphate (LFP) cathodes (PS: production scraps, EOL: end-of-life).
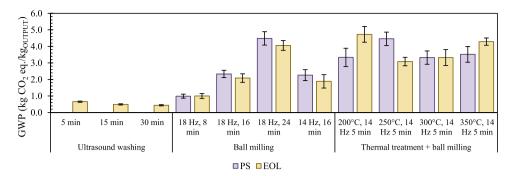
Fig. 10. Global warming impact (GWP$_{100}$) associated to the pre-treatment processes applied to lithium iron phosphate (LFP) cathodes (PS: production scraps, EOL: end-of-life).

washing was directly related to the process duration, the specific energy consumption per kg of detached cathode material was greater when the process duration was shorter.

Water was required for ultrasonic washing as 20 kg of water per 1 kg of samples. Considering the separation rates of EOL samples by ultrasound washing, water consumption was: 59.20 kg of water for each kg of detached cathode powder after 5 min, 42.29 kg after 15 min and 37.00 kg after 30 min.

The environmental impacts due to energy and water consumption for the compared pre-treatments (Appendix, Table A8 and Table A9) are compared in Fig. 10. Ultrasounds washing denoted the lowest impact due to the limited energy demand. Energy consumption was the main contribution to most of considered impact categories: 98.67% of global warming, 82.30% of terrestrial acidification, 84.50% of freshwater eutrophication, 92.53% carcinogenic human toxicity and 82.23% of non-carcinogenic human toxicity. The additional contribution due to the use of water was significant only in the category of "water consumption", where it accounted to 55.6%.

Considering the detachment of cathode material from current collector through thermal treatment followed by ball milling, the best performing conditions have been identified in: thermal treatment at 200 °C for PS samples and at 250 °C for EOL samples. The global warming impact associated with those treatment was: 3.33 ± 0.55 kg CO$_2$ eq. /kg of detached cathode material for PS samples and 3.08 ± 0.25 kg CO$_2$ eq. /kg of detached cathode material for EOL samples.

The direct comparison between the separation efficiency of the considered physical pre-treatments and the process conventionally applied (i.e., solvent extraction) for the detachment of cathode active material from the current collector is outside the scope of this study. However, to have a reference, the overall environmental impacts calculated for the physical detachment methods proposed in this study have been compared with the impacts of conventional solvents manufacturing reported by literature. Conventional detachment methods require the use of solvents such as acetone, acetonitrile, and dimethyl carbonate (DMC), with a ratio of 10 kg of solvents per 1 kg of cathodes [68]. The global warming impact potentially associated with the production of solvents [62] was estimated as 26.22 kg CO$_2$ eq/kg of cathodes for acetone; 50.31 kg CO$_2$ eq/kg of cathodes for acetonitrile: and 22.69 kg CO$_2$ eq/kg of cathodes for DMC. Thus, the use of solvent-free pre-treatment processes for the detachment of cathode active powder, as proposed by this study, could lower the global warming impact by an order of magnitude.

The operative costs associated to the considered pre-treatments have been accounted based on the cost of energy and water. Because of the low energy consumption and limited cost of water, the costs of ultrasound washing were the lowest: 0.28 ± 0.02 €/kg of detached cathode material after 5 min, 0.21 ± 0.02 €/kg of detached cathode material after 15 min, 0.19 ± 0.02 €/kg of detached cathode material after 30 min. Ball milling required higher operative costs increasing the duration of the treatment: from a minimum of 0.43 ± 0.05 €/kg for PS

samples and 0.44 ± 0.06 €/kg for EOL samples after 8 min at 1080 rpm to a maximum of 1.95 ± 0.18 €/kg for PS samples and 1.77 ± 0.13 €/kg for EOL samples after 24 min at 1080 rpm. Cost associated with ball milling at 1080 rpm for 16 min (1.02 ± 0.10 €/kg for PS samples and 0.91 ± 0.11 €/kg for EOL samples) was comparable with the cost of ball milling at 840 rpm for the same time (0.98 ± 0.14 €/kg for PS samples and 0.82 ± 0.18 €/kg for EOL samples). Lastly, the cost of thermal treatment followed by ball milling followed the same pattern of energy consumption. The cost associated with PS samples were as follows: 1.45 ± 0.24 €/kg of detached cathode material when the temperature of the thermal treatment was 200 °C, 1.94 ± 0.18 €/kg at 250 °C, 1.45 ± 0.18 €/kg at 300 °C and 1.53 ± 0.18 €/kg at 350 °C. The costs of thermal treatment followed by ball milling for EOL samples were: 2.06 ± 0.21 €/kg at 200 °C, 1.34 ± 0.11 €/kg at 250 °C, 1.45 ± 0.21 €/kg at 300 °C and 1.87 ± 0.10 €/kg at 350 °C. The cost associated with these detachment methods were between 1% and 10% of the market values of commercial LFP powder (20.041 €/kg) [62], leaving economic margin for further recycling processes.

4. Conclusions

Pre-treatment processes aimed at mechanical detachment of the active cathode material from current collector have been compared in this study on PS and EOL cathodes from LFP batteries, in terms of technical performance, environmental impact and economic cost. All processes performed better on EOL samples than on PS samples, both in terms of separation rate and material loss. Ultrasound washing, especially, was unsuccessful for the detachment of cathode material from PS samples. For both PS and EOL the best results were achieved by thermal treatment and ball milling.

Higher milling frequency improved separation efficiency of Li (r^2 =94% for PS and r^2 =88% for EOL samples), Fe (r^2 =82% for both PS and EOL samples) and P (r^2 =88% for PS and r^2 =48% for EOL samples). Instead, increasing the duration of milling processes caused higher Al impurities both in PS samples (r^2 =86%) and EOL samples (r^2 =76%). A significant difference between PS and EOL samples was ascribed to the degradation of the binder. PS cathodes have never been cycled, and the bond between cathode material and current collector was stronger; thus some Li, Fe and P remained attached to current collectors after pre-treatments. EOL samples instead underwent deterioration of the binder during the battery lifetime; during pre-treatment, separation of the cathode material was easier and material loss was due to the fine fraction generated by ball milling.

The highest separation efficiencies were obtained by low intensity (840 rpm) ball milling for short time (5 min) with prior thermal treatment for 30 min at 200 °C for PS samples, and 250 °C for EOL samples; 95 ± 5% of Li, 99 ± 6% of Fe, and 80 ± 3% of P were recovered from PS samples and 93 ± 15% of Li, 97 ± 21% of Fe and 82 ± 20% of P were recovered from EOL samples. Besides, Al impurities were limited to 0.05% for PS samples and to 0.13% for EOL samples.

Environmental impacts were estimated based on energy and water consumption during pre-treatments. The best performing processes caused a global warming impact of: 3.33 ± 0.55 kg CO2 eq/kg of detached cathode material for PS samples, and 3.08 ± 0.25 kg CO2 eq/kg of detached cathode material for EOL samples. As a reference, according to literature the global warming impact due to the application of chemical solvents for binder dissolution is greater by one order of magnitude.

The costs associated with the best pre-treatment were 1.45 ± 0.24 €/kg for PS samples and 1.34 ± 0.11 €/kg for EOL samples. Besides, the costs associated with the other detachment methods were below 10% of commercial LFP market value.

In conclusion, an effective detachment of LFP cathode material from current collectors based on limited energy demand and solvent-free methods seems possible. Thermal pre-treatment is recommended to increase the overall process efficiencies, and long milling times should be avoided to limit the amount of Al impurities and energy demand (and subsequently the environmental impacts and operative costs) without producing a significant effect on separation efficiency.

CRediT authorship contribution statement

Fiore Silvia: Conceptualization, Methodology, Supervision, Writing

– review & editing. **Bruno Martina:** Conceptualization, Data curation, Investigation, Visualization, Writing – original draft.

Declaration of Competing Interest

The authors declare that they have no known competing financial interests or personal relationships that could have appeared to influence the work reported in this paper.

Data availability

Data will be made available on request.

Acknowledgments

Appendix

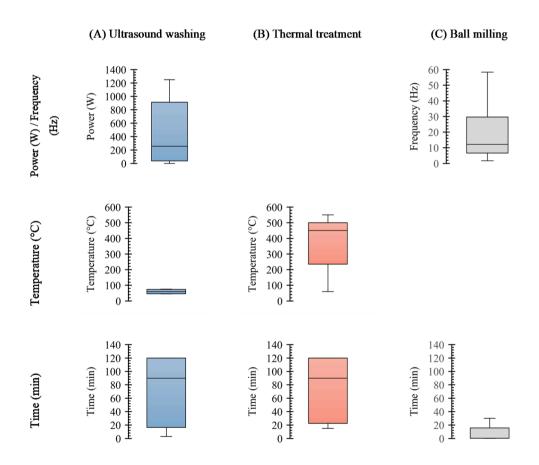**Fig. A1.** Operative conditions (ultrasound power and milling frequency; temperature and time) applied for (A) ultrasound washing, (B) thermal treatment and (C) ball milling applied as pre-treatment for battery recycling, according to literature (box: interquartile range between 25th and 75th percentile, middle line: median, whiskers: values within one standard deviation of either side of the median).

.

Fig. A2. Equipment applied during experimental activity: (A) Bandelin SONOREX DIGIPLUS DL 514 BH ultrasonic bath ultrasonic, (B) ARGO LAB TCN 30 oven, (C) ZE muffle furnace, (D) Retsch MM200 ball mill.

Fig. A3. Composition of production scraps (PS) and end of life (EOL) lithium iron phosphate cathodes measured in this study compared with literature [64,66].

Fig. A4. Weight loss (%) for production scraps and end of life cathodes.

Table A1
Impact categories considered in the environmental assessment.

Impact category	Abbreviation	unit of measure
Acidification: terrestrial	TAP	kg SO_2-eq
Climate change	GWP100	kg CO_2-eq
Ecotoxicity: freshwater	FETP	kg 1,4-DCB-eq
Ecotoxicity: marine	METP	kg 1,4-DCB-eq
Ecotoxicity: terrestrial	TETP	kg 1,4-DCB-eq
Energy resources: non-renewable, fossil	FFP	kg oil-eq
Eutrophication: freshwater	FEP	kg P-eq
Eutrophication: marine	MEP	kg N-eq
Human toxicity: carcinogenic	HTP_c	kg 1,4-DCB-eq
Human toxicity: non-carcinogenic	HTP_{nc}	kg 1,4-DCB-eq
Ionising radiation	IRP	kBq Co-60-eq
Land use	LOP	m^2·a crop-eq
Material resources: metals/minerals	SOP	kg Cu-eq
Ozone depletion	$ODP_{infinite}$	kg CFC-11-eq
Particulate matter formation	PMFP	kg $PM_{2.5}$.eq
Photochemical oxidant formation human health	HOFP	kg NO_x.eq
Photochemical oxidant formation: terrestrial ecosystems	EOFP	kg NO_x.eq
Water use	WCP	m^3

Table A2
Efficiency of ultrasound washing for detachment of cathode material from current collectors.

Ultrasound washing	Production scraps			End of life		
Time (min)	Separation rate Li (%)	Separation rate Fe (%)	Separation rate P (%)	Separation rate Li (%)	Separation rate Fe (%)	Separation rate P (%)
5	-	-		$30 \pm 5\%$	$32\% \pm 5\%$	$36\% \pm 6\%$
15	-	-		$41 \pm 9\%$	$55\% \pm 9\%$	$61\% \pm 10\%$
30	-	-		$50 \pm 6\%$	$76\% \pm 13\%$	$69\% \pm 11\%$

Table A3
Efficiency of ball milling for detachment of cathode material from current collectors.

Ball milling		Production scraps			End of life		
Frequency (Hz)	Time (min)	Separation rate Li (%)	Separation rate Fe (%)	Separation rate P (%)	Separation rate Li (%)	Separation rate Fe (%)	Separation rate P (%)
18	8	$93 \pm 6\%$	$84\% \pm 5\%$	$66\% \pm 5\%$	$96 \pm 12\%$	$96\% \pm 17\%$	$67\% \pm 16\%$
18	16	$74 \pm 8\%$	$48\% \pm 11\%$	$46\% \pm 6\%$	$99 \pm 15\%$	$98\% \pm 28\%$	$70\% \pm 16\%$
18	24	$74 \pm 7\%$	$54\% \pm 6\%$	$50\% \pm 5\%$	$74 \pm 20\%$	$96\% \pm 22\%$	$73\% \pm 14\%$
14	16	$68 \pm 2\%$	$50\% \pm 4\%$	$42\% \pm 3\%$	$97 \pm 13\%$	$79\% \pm 18\%$	$58\% \pm 16\%$

Table A4
Efficiency of thermal treatment and ball milling for detachment of cathode material from current collectors.

Thermal treatment – Ball milling (14 Hz, 5 min)	Production scraps			End of life		
Temperature (°C)	Separation rate Li (%)	Separation rate Fe (%)	Separation rate P (%)	Separation rate Li (%)	Separation rate Fe (%)	Separation rate P (%)
200	$95 \pm 5\%$	$99\% \pm 6\%$	$80\% \pm 3\%$	$72 \pm 11\%$	$73\% \pm 16\%$	$54\% \pm 10\%$
250	$66 \pm 4\%$	$86\% \pm 5\%$	$67\% \pm 6\%$	$93 \pm 15\%$	$97\% \pm 21\%$	$82\% \pm 20\%$
300	$85 \pm 2\%$	$81\% \pm 3\%$	$63\% \pm 21\%$	$87 \pm 16\%$	$97\% \pm 22\%$	$90\% \pm 21\%$
350	$91 \pm 7\%$	$83\% \pm 8\%$	$67\% \pm 12\%$	$67 \pm 11\%$	$89\% \pm 16\%$	$69\% \pm 12\%$

Table A5
Pearson's correlation coefficient between operative parameters and KPIs for PS samples (colour scale: blue = positive correlation; red = negative correlation; white = no correlation).

	Separation rate Li (%)	Separation rate Fe (%)	Separation rate P (%)	Material loss (%)	Al impurities (%)
Ultrasound washing: time (min)	-78%	-72%	-76%	-70%	-51%
Thermal treatment: temperature (°C)	50%	66%	62%	28%	4%
Ball milling: frequency (Hz)	94%	82%	88%	82%	69%
Ball milling: time (min)	51%	26%	36%	76%	86%
Separation rate Li (%)		94%	97%	72%	49%
Separation rate Fe (%)			99%	69%	41%
Separation rate P (%)				63%	32%
Material loss (%)					74%

Table A6

Pearson's correlation coefficient between operative parameters and KPIs for EOL samples (colour scale: blue= positive correlation; red= negative correlation; white= no correlation).

	Separation rate Li (%)	Separation rate Fe (%)	Separation rate P (%)	Material loss (%)	Al impurities (%)
Ultrasound washing: time (min)	-60%	-38%	-11%	42%	-3%
Thermal treatment: temperature (°C)	17%	35%	46%	-24%	-29%
Ball milling: frequency (Hz)	88%	82%	48%	-76%	23%
Ball milling: time (min)	61%	54%	23%	-40%	76%
Separation rate Li (%)		84%	57%	-89%	11%
Separation rate Fe (%)			85%	-90%	24%
Separation rate P (%)				-78%	21%
Material loss (%)					2%

Table A7

Energy and water demands for alternative separation technologies (functional unit: 1 kg of treated cathodes).

Detachment method	Energy consumption kWh/kg_{INPUT}	Water consumption kg_{water}/kg_{INPUT}
Ultrasound washing: 5 min	0.585	34.63
Ultrasound washing: 15 min	0.615	26.01
Ultrasound washing:30 min	0.625	23.13
Ball milling: 18 Hz, 8 min	2.25	0
Ball milling: 18 Hz, 16 min	4	0
Ball milling: 18 Hz, 24 min	7	0
Ball milling: 14 Hz, 16 min	3.25	0
Thermal treatment: 200 °C - Ball milling: 14 Hz, 5 min	6.75	0
Thermal treatment: 250 °C - Ball milling: 14 Hz, 5 min	6.75	0
Thermal treatment: 300 °C - Ball milling: 14 Hz, 5 min	6.75	0
Thermal treatment: 350 °C - Ball milling: 14 Hz, 5 min	6.75	0

Table A8

Environmental impacts of ball milling for PS and EOL samples.

Indicator	Production scrap				End of Life				unit of measure
	18 Hz, 8 min	18 Hz, 16 min	18 Hz, 24 min	14 Hz, 16 min	18 Hz, 8 min	18 Hz, 16 min	18 Hz, 24 min	14 Hz, 16 min	
TAP	$3.85 \cdot 10^{-3}$	$9.08 \cdot 10^{-3}$	$1.75 \cdot 10^{-2}$	$8.80 \cdot 10^{-3}$	$3.90 \cdot 10^{-3}$	$8.11 \cdot 10^{-3}$	$1.58 \cdot 10^{-2}$	$7.34 \cdot 10^{-3}$	kg SO_2-eq
GWP100	$9.90 \cdot 10^{-1}$	2.33	4.48	2.26	1.00	2.08	4.06	1.88	kg CO_2-eq
FETP	$1.22 \cdot 10^{-1}$	$2.88 \cdot 10^{-1}$	$5.54 \cdot 10^{-1}$	$2.79 \cdot 10^{-1}$	$1.24 \cdot 10^{-1}$	$2.57 \cdot 10^{-1}$	$5.01 \cdot 10^{-1}$	$2.33 \cdot 10^{-1}$	kg 1,4-DCB-eq

Table A8 (*continued*)

Indicator	Production scrap				End of Life				unit of measure
	18 Hz, 8 min	18 Hz, 16 min	18 Hz, 24 min	14 Hz, 16 min	18 Hz, 8 min	18 Hz, 16 min	18 Hz, 24 min	14 Hz, 16 min	
METP	$1.55 \cdot 10^{-1}$	$3.65 \cdot 10^{-1}$	$7.03 \cdot 10^{-1}$	$3.54 \cdot 10^{-1}$	$1.57 \cdot 10^{-1}$	$3.26 \cdot 10^{-1}$	$6.36 \cdot 10^{-1}$	$2.95 \cdot 10^{-1}$	kg 1,4-DCB-eq
TETP	5.88	$1.39 \cdot 10^{1}$	$2.66 \cdot 10^{1}$	$1.34 \cdot 10^{1}$	5.94	$1.24 \cdot 10^{1}$	$2.41 \cdot 10^{1}$	$1.12 \cdot 10^{1}$	kg 1,4-DCB-eq
FFP	$2.69 \cdot 10^{-1}$	$6.35 \cdot 10^{-1}$	1.22	$6.15 \cdot 10^{-1}$	$2.72 \cdot 10^{-1}$	$5.67 \cdot 10^{-1}$	1.10	$5.13 \cdot 10^{-1}$	kg oil-eq
FEP	$9.16 \cdot 10^{-4}$	$2.16 \cdot 10^{-3}$	$4.15 \cdot 10^{-3}$	$2.09 \cdot 10^{-3}$	$9.27 \cdot 10^{-4}$	$1.93 \cdot 10^{-3}$	$3.76 \cdot 10^{-3}$	$1.74 \cdot 10^{-3}$	kg P-eq
MEP	$6.77 \cdot 10^{-5}$	$1.59 \cdot 10^{-4}$	$3.07 \cdot 10^{-4}$	$1.54 \cdot 10^{-4}$	$6.84 \cdot 10^{-5}$	$1.42 \cdot 10^{-4}$	$2.77 \cdot 10^{-4}$	$1.29 \cdot 10^{-4}$	kg N-eq
HTP$_c$	$6.99 \cdot 10^{-2}$	$1.65 \cdot 10^{-1}$	$3.17 \cdot 10^{-1}$	$1.59 \cdot 10^{-1}$	$7.07 \cdot 10^{-2}$	$1.47 \cdot 10^{-1}$	$2.87 \cdot 10^{-1}$	$1.33 \cdot 10^{-1}$	kg 1,4-DCB-eq
HTP$_{nc}$	1.87	4.40	8.45	4.26	1.89	3.92	7.65	3.55	kg 1,4-DCB-eq
IRP	$5.68 \cdot 10^{-1}$	1.34	2.58	1.30	$5.75 \cdot 10^{-1}$	1.20	2.33	1.08	kBq Co-60-eq
LOP	$3.17 \cdot 10^{-2}$	$7.47 \cdot 10^{-2}$	$1.44 \cdot 10^{-1}$	$7.23 \cdot 10^{-2}$	$3.20 \cdot 10^{-2}$	$6.67 \cdot 10^{-2}$	$1.30 \cdot 10^{-1}$	$6.03 \cdot 10^{-2}$	m^2·a crop-eq
SOP	$8.75 \cdot 10^{-3}$	$2.06 \cdot 10^{-2}$	$3.96 \cdot 10^{-2}$	$2.00 \cdot 10^{-2}$	$8.84 \cdot 10^{-3}$	$1.84 \cdot 10^{-2}$	$3.59 \cdot 10^{-2}$	$1.66 \cdot 10^{-2}$	kg Cu-eq
ODP$_{infinite}$	$4.55 \cdot 10^{-7}$	$1.07 \cdot 10^{-6}$	$2.06 \cdot 10^{-6}$	$1.04 \cdot 10^{-6}$	$4.60 \cdot 10^{-7}$	$9.57 \cdot 10^{-7}$	$1.86 \cdot 10^{-6}$	$8.66 \cdot 10^{-7}$	kg CFC-11-eq
PMFP	$1.52 \cdot 10^{-3}$	$3.58 \cdot 10^{-3}$	$6.87 \cdot 10^{-3}$	$3.46 \cdot 10^{-3}$	$1.53 \cdot 10^{-3}$	$3.19 \cdot 10^{-3}$	$6.22 \cdot 10^{-3}$	$2.89 \cdot 10^{-3}$	kg PM$_{2.5}$.eq
HOFP	$1.83 \cdot 10^{-3}$	$4.32 \cdot 10^{-3}$	$8.30 \cdot 10^{-3}$	$4.18 \cdot 10^{-3}$	$1.85 \cdot 10^{-3}$	$3.85 \cdot 10^{-3}$	$7.51 \cdot 10^{-3}$	$3.49 \cdot 10^{-3}$	kg NO$_x$.eq
EOFP	$1.89 \cdot 10^{-3}$	$4.46 \cdot 10^{-3}$	$8.57 \cdot 10^{-3}$	$4.32 \cdot 10^{-3}$	$1.91 \cdot 10^{-3}$	$3.98 \cdot 10^{-3}$	$7.76 \cdot 10^{-3}$	$3.60 \cdot 10^{-3}$	kg NO$_x$.eq
WCP	$1.24 \cdot 10^{-2}$	$2.93 \cdot 10^{-2}$	$5.63 \cdot 10^{-2}$	$2.84 \cdot 10^{-2}$	$1.26 \cdot 10^{-2}$	$2.62 \cdot 10^{-2}$	$5.10 \cdot 10^{-2}$	$2.37 \cdot 10^{-2}$	m^3

Table A9

Environmental impacts of thermal treatment followed by ball milling for PS and EOL samples.

Indicator	Production scrap				End of Life				unit of measure
	200 °C	250 °C	300 °C	350 °C	200 °C	250 °C	300 °C	350 °C	
TAP	$1.30 \cdot 10^{-2}$	$1.74 \cdot 10^{-2}$	$1.29 \cdot 10^{-2}$	$1.37 \cdot 10^{-2}$	$1.84 \cdot 10^{-2}$	$1.20 \cdot 10^{-2}$	$1.29 \cdot 10^{-2}$	$1.67 \cdot 10^{-2}$	kg SO$_2$-eq
GWP100	3.33	4.46	3.32	3.52	4.73	3.08	3.32	4.29	kg CO$_2$-eq
FETP	$4.12 \cdot 10^{-1}$	$5.51 \cdot 10^{-1}$	$4.10 \cdot 10^{-1}$	$4.34 \cdot 10^{-1}$	$5.84 \cdot 10^{-1}$	$3.81 \cdot 10^{-1}$	$4.10 \cdot 10^{-1}$	$5.30 \cdot 10^{-1}$	kg 1,4-DCB-eq
METP	$5.22 \cdot 10^{-1}$	$6.99 \cdot 10^{-1}$	$5.20 \cdot 10^{-1}$	$5.51 \cdot 10^{-1}$	$7.41 \cdot 10^{-1}$	$4.83 \cdot 10^{-1}$	$5.21 \cdot 10^{-1}$	$6.72 \cdot 10^{-1}$	kg 1,4-DCB-eq
TETP	$1.98 \cdot 10^{1}$	$2.65 \cdot 10^{1}$	$1.97 \cdot 10^{1}$	$2.09 \cdot 10^{1}$	$2.81 \cdot 10^{1}$	$1.83 \cdot 10^{1}$	$1.97 \cdot 10^{1}$	$2.55 \cdot 10^{1}$	kg 1,4-DCB-eq
FFP	$9.07 \cdot 10^{-1}$	1.21	$9.03 \cdot 10^{-1}$	$9.57 \cdot 10^{-1}$	1.29	$8.39 \cdot 10^{-1}$	$9.04 \cdot 10^{-1}$	1.17	kg oil-eq
FEP	$3.09 \cdot 10^{-3}$	$4.13 \cdot 10^{-3}$	$3.07 \cdot 10^{-3}$	$3.26 \cdot 10^{-3}$	$4.38 \cdot 10^{-3}$	$2.85 \cdot 10^{-3}$	$3.08 \cdot 10^{-3}$	$3.97 \cdot 10^{-3}$	kg P-eq
MEP	$2.28 \cdot 10^{-4}$	$3.05 \cdot 10^{-4}$	$2.27 \cdot 10^{-4}$	$2.40 \cdot 10^{-4}$	$3.23 \cdot 10^{-4}$	$2.11 \cdot 10^{-4}$	$2.27 \cdot 10^{-4}$	$2.93 \cdot 10^{-4}$	kg N-eq
HTP$_c$	$2.35 \cdot 10^{-1}$	$3.15 \cdot 10^{-1}$	$2.34 \cdot 10^{-1}$	$2.48 \cdot 10^{-1}$	$3.34 \cdot 10^{-1}$	$2.18 \cdot 10^{-1}$	$2.35 \cdot 10^{-1}$	$3.03 \cdot 10^{-1}$	kg 1,4-DCB-eq
HTP$_{nc}$	6.28	8.40	6.25	6.63	8.91	5.81	6.26	8.08	kg 1,4-DCB-eq
IRP	1.91	2.56	1.91	2.02	2.71	1.77	1.91	2.46	kBq Co-60-eq
LOP	$1.07 \cdot 10^{-1}$	$1.43 \cdot 10^{-1}$	$1.06 \cdot 10^{-1}$	$1.13 \cdot 10^{-1}$	$1.51 \cdot 10^{-1}$	$9.87 \cdot 10^{-2}$	$1.06 \cdot 10^{-1}$	$1.37 \cdot 10^{-1}$	m^2·a crop-eq
SOP	$2.95 \cdot 10^{-2}$	$3.94 \cdot 10^{-2}$	$2.93 \cdot 10^{-2}$	$3.11 \cdot 10^{-2}$	$4.18 \cdot 10^{-2}$	$2.72 \cdot 10^{-2}$	$2.94 \cdot 10^{-2}$	$3.79 \cdot 10^{-2}$	kg Cu-eq
ODP$_{infinite}$	$1.53 \cdot 10^{-6}$	$2.05 \cdot 10^{-6}$	$1.53 \cdot 10^{-6}$	$1.62 \cdot 10^{-6}$	$2.17 \cdot 10^{-6}$	$1.42 \cdot 10^{-6}$	$1.53 \cdot 10^{-6}$	$1.97 \cdot 10^{-6}$	kg CFC-11-eq
PMFP	$5.11 \cdot 10^{-3}$	$6.83 \cdot 10^{-3}$	$5.09 \cdot 10^{-3}$	$5.39 \cdot 10^{-3}$	$7.25 \cdot 10^{-3}$	$4.73 \cdot 10^{-3}$	$5.09 \cdot 10^{-3}$	$6.58 \cdot 10^{-3}$	kg PM$_{2.5}$-eq
HOFP	$6.17 \cdot 10^{-3}$	$8.25 \cdot 10^{-3}$	$6.14 \cdot 10^{-3}$	$6.51 \cdot 10^{-3}$	$8.75 \cdot 10^{-3}$	$5.70 \cdot 10^{-3}$	$6.15 \cdot 10^{-3}$	$7.94 \cdot 10^{-3}$	kg NO$_x$-eq
EOFP	$6.37 \cdot 10^{-3}$	$8.52 \cdot 10^{-3}$	$6.34 \cdot 10^{-3}$	$6.72 \cdot 10^{-3}$	$9.04 \cdot 10^{-3}$	$5.89 \cdot 10^{-3}$	$6.35 \cdot 10^{-3}$	$8.20 \cdot 10^{-3}$	kg NO$_x$-eq
WCP	$4.19 \cdot 10^{-2}$	$5.60 \cdot 10^{-2}$	$4.17 \cdot 10^{-2}$	$4.42 \cdot 10^{-2}$	$5.94 \cdot 10^{-2}$	$3.87 \cdot 10^{-2}$	$4.17 \cdot 10^{-2}$	$5.39 \cdot 10^{-2}$	m^3

References

[1] Statista, Projected global battery demand by application, (2021). https://www.statista.com/statistics/1103218/global-battery-demand-forecast/ (accessed March 28, 2023).

[2] M. Neidhardt, J. Mas-Peiro, M. Schulz-Moenninghoff, J.O. Pou, R. Gonzalez-Olmos, A. Kwade, B. Schmuelling, Forecasting the global battery material flow: analyzing the break-even points at which secondary battery raw materials can substitute primary materials in the battery production, Appl. Sci. 12 (2022), https://doi.org/10.3390/app12094790.

[3] G. Mishra, R. Jha, A. Meshram, K.K. Singh, A review on recycling of lithium-ion batteries to recover critical metals, J. Environ. Chem. Eng. 10 (2022) 108534, https://doi.org/10.1016/j.jece.2022.108534.

[4] J. Dunn, M. Slattery, A. Kendall, H. Ambrose, S. Shen, Circularity of lithium-ion battery materials in electric vehicles, Environ. Sci. Technol. 55 (2021) 5189–5198. ⟨https://pubs.acs.org/doi/10.1021/acs.est.0c07030⟩.

[5] M. Bruno, S. Fiore, Material flow analysis of lithium-ion battery recycling in europe: environmental and economic implications, Batteries 9 (2023), https://doi.org/10.3390/batteries9040231.

[6] Z.A. Kader, A. Marshall, J. Kennedy, A review on sustainable recycling technologies for lithium-ion batteries, Emergent Mater. 4 (2021) 725–735, https://doi.org/10.1007/s42247-021-00201-w.

[7] C. Aichberger, G. Jungmeier, Environmental life cycle impacts of automotive batteries based on a literature review, Energies 13 (2020) 6345, https://doi.org/10.3390/en13236345.

[8] E. Mossali, N. Picone, L. gentilini, O. Rodrìguez, J.M. Pérez, M. Colledani, Lithium-ion batteries towards circular economy: a literature review of opportunities and issues of recycling treatments, J. Environ. Manag. 264 (2020) 110500, https://doi.org/10.1016/j.jenvman.2020.110500.

[9] X. Wang, G. Gaustad, C.W. Babbitt, K. Richa, Economies of scale for future lithium-ion battery recycling infrastructure, Resour. Conserv. Recycl. 83 (2014) 53–62, https://doi.org/10.1016/j.resconrec.2013.11.009.

[10] L. Brückner, J. Frank, T. Elwert, Industrial recycling of lithium-ion batteries—a critical review of metallurgical process routes, Metals (Basel) 10 (2020) 1–29, https://doi.org/10.3390/met10081107.

[11] D. Latini, M. Vaccari, M. Lagnoni, M. Orefice, F. Mathieux, J. Huisman, L. Tognotti, A. Bertei, A comprehensive review and classification of unit operations with assessment of outputs quality in lithium-ion battery recycling, J. Power Sources 546 (2022) 231979, https://doi.org/10.1016/j.jpowsour.2022.231979.

[12] R. Sommerville, J. Shaw-Stewart, V. Goodship, N. Rowson, E. Kendrick, A review of physical processes used in the safe recycling of lithium ion batteries, Sustain. Mater. Technol. 25 (2020) e00197, https://doi.org/10.1016/j.susmat.2020.e00197.

[13] V.C.I. Takahashi, A.B. Botelho Junior, D.C.R. Espinosa, J.A.S. Tenório, Enhancing cobalt recovery from Li-ion batteries using grinding treatment prior to the leaching and solvent extraction process, J. Environ. Chem. Eng. 8 (2020) 103801, https://doi.org/10.1016/j.jece.2020.103801.

[14] I. Sultana, Y. Chen, S. Huang, M.M. Rahman, Recycled value-added circular energy materials for new battery application: recycling strategies, challenges, and sustainability-a comprehensive review, J. Environ. Chem. Eng. 10 (2022) 108728, https://doi.org/10.1016/j.jece.2022.108728.

[15] H. Li, S. Xing, Y. Liu, F. Li, H. Guo, G. Kuang, Recovery of lithium, iron, and phosphorus from spent LiFePO4 batteries using stoichiometric sulfuric acid leaching system, ACS Sustain. Chem. Eng. 5 (2017) 8017–8024. ⟨https://pubs.acs.org/doi/10.1021/acssuschemeng.7b01594⟩.

[16] H. Li, H. Ye, M. Sun, W. Chen, Process for recycle of spent lithium iron phosphate battery via a selective leaching-precipitation method, J. Cent. South Univ. 27 (2020) 3239–3248, https://doi.org/10.1007/s11771-020-4543-3.

[17] H. Tang, X.I. Dai, Q. Li, Y. Qiao, F. Tan, Selective leaching of LiFePO4 by H2SO4 in the presence of NaClO3, Rev. Chim. 71 (2020) 248–254, https://doi.org/10.37358/RC.20.7.8242.

[18] X. Qin, G. Yang, F. Cai, B. Wang, B. Jiang, H. Chen, C. Tan, Recovery and reuse of spent LiFePO4 batteries, J. New Mater. Electrochem. Syst. 22 (2019) 119–124, https://doi.org/10.14447/jnmes.v22i3.a01.

[19] K. Liu, M. Wang, Q. Zhang, Z. Xu, C. Labianca, M. Komárek, B. Gao, D.C.W. Tsang, A perspective on the recovery mechanisms of spent lithium iron phosphate cathode materials in different oxidation environments, J. Hazard. Mater. 445 (2023), https://doi.org/10.1016/j.jhazmat.2022.130502.

[20] P. Yadav, C.J. Jie, S. Tan, M. Srinivasan, Recycling of cathode from spent lithium iron phosphate batteries, J. Hazard. Mater. 399 (2020) 123068, https://doi.org/10.1016/j.jhazmat.2020.123068.

[21] H. Bi, H. Zhu, J. Zhan, L. Zu, Y. Bai, H. Li, Environmentally friendly automated line for recovering aluminium and lithium iron phosphate components of spent lithium-iron phosphate batteries, Waste Manag. Res. 39 (2021) 1164–1173. ⟨https://journals.sagepub.com/doi/10.1177/0734242×20982060⟩.

[22] O. Buken, K. Mancini, A. Sarkar, A sustainable approach to cathode delamination using a green solvent, RSC Adv. 11 (2021) 27356, https://doi.org/10.1039/D1RA04922D.

[23] Q. Liang, H. Yue, S. Wang, S. Yang, K.-H. Lam, X. Hou, Recycling and crystal regeneration of commercial used LiFePO4 cathode materials, Electrochim. Acta 330 (2020), https://doi.org/10.1016/j.electacta.2019.135323.

[24] S.D. Widijatmoko, F. Gu, Z. Wang, P. Hall, Selective liberation in dry milled spent lithium-ion batteries, Sustain. Mater. Technol. 23 (2020), https://doi.org/10.1016/j.susmat.2019.e00134.

[25] N. Vieceli, R. Casasola, G. Lombardo, B. Ebin, M. Petranikova, Hydrometallurgical recycling of EV lithium-ion batteries: Effects of incineration on the leaching efficiency of metals using sulfuric acid, Waste Manag 125 (2021) 192–203, https://doi.org/10.1016/j.wasman.2021.02.039.

[26] C. Hanisch, T. Loellhoeffel, J. Diekmann, K.J. Markley, W. Haselrieder, A. Kwade, Recycling of lithium-ion batteries: A novel method to separate coating and foil of electrodes, J. Clean. Prod. 108 (2015) 301–311, https://doi.org/10.1016/j.jclepro.2015.08.026.

[27] M. Jafari, M.M. Torabian, A. Bazargan, A facile chemical-free cathode powder separation method for lithium ion battery resource recovery, J. Energy Storage 31 (2020), https://doi.org/10.1016/j.est.2020.101564.

[28] J. Xie, K. Huang, Z. Nie, W. Yuan, X. Wang, Q. Song, X. Zhang, C. Zhang, J. Wang, J.C. Crittenden, An effective process for the recovery of valuable metals from cathode material of lithium-ion batteries by mechanochemical reduction, Resour. Conserv. Recycl. 168 (2021) 105261, https://doi.org/10.1016/j.resconrec.2020.105261.

[29] L.P. He, S.Y. Sun, X.F. Song, J.G. Yu, Recovery of cathode materials and Al from spent lithium-ion batteries by ultrasonic cleaning, Waste Manag. 46 (2015) 523–528, https://doi.org/10.1016/j.wasman.2015.08.035.

[30] C. Lei, I. Aldous, J.M. Hartley, D.L. Thompson, S. Scott, R. Hanson, P.A. Anderson, E. Kendrick, R. Sommerville, K.S. Ryder, A.P. Abbott, Lithium ion battery recycling using high-intensity ultrasonication, Green. Chem. 23 (2021) 4710–4715, https://doi.org/10.1039/d1gc01623g.

[31] G. Zhang, Y. He, Y. Feng, H. Wang, X. Zhu, Pyrolysis-ultrasonic-assisted flotation technology for recovering graphite and LiCoO2 from spent lithium-ion batteries, ACS Sustain. Chem. Eng. 6 (2018) 10896–10904. ⟨https://pubs.acs.org/doi/full/10.1021/acssuschemeng.8b02186?src=recsys⟩.

[32] J. Li, P. Shi, Z. Wang, Y. Chen, C. Chang, A combined recovery process of metals in spent lithium-ion batteries, Chemosphere 77 (2009) 1132–1136, https://doi.org/10.1016/j.chemosphere.2009.08.040.

[33] L. Yang, G. Xi, Y. Xi, Recovery of Co, Mn, Ni, and Li from spent lithium ion batteries for the preparation of LiNixCoyMnzO2 cathode materials, Ceram. Int. 41 (2015) 11498–11503, https://doi.org/10.1016/j.ceramint.2015.05.115.

[34] S. Zhao, W. Zhang, G. Li, H. Zhu, J. Huang, W. He, Ultrasonic renovating and coating modifying spent lithium cobalt oxide from the cathode for the recovery and sustainable utilization of lithium-ion battery, J. Clean. Prod. 257 (2020), https://doi.org/10.1016/j.jclepro.2020.120510.

[35] F. Jiang, Y. Chen, S. Ju, Q. Zhu, L. Zhang, J. Peng, X. Wang, J.D. Miller, Ultrasound-assisted leaching of cobalt and lithium from spent lithium-ion batteries, Ultrason. Sonochem. 48 (2018) 88–95, https://doi.org/10.1016/j.ultsonch.2018.05.019.

[36] X. Chen, S. Li, X. Wu, T. Zhou, H. Ma, In-situ recycling of coating materials and Al foils from spent lithium ion batteries by ultrasonic-assisted acid scrubbing, J. Clean. Prod. 258 (2020), https://doi.org/10.1016/j.jclepro.2020.120943.

[37] R. Golmohammadzadeh, F. Rashchi, E. Vahidi, Recovery of lithium and cobalt from spent lithium-ion batteries using organic acids: Process optimization and kinetic aspects, Waste Manag. 64 (2017) 244–254, https://doi.org/10.1016/j.wasman.2017.03.037.

[38] L. Li, L. Zhai, X. Zhang, J. Lu, R. Chen, F. Wu, K. Amine, Recovery of valuable metals from spent lithium-ion batteries by ultrasonic-assisted leaching process, J. Power Sources 262 (2014) 380–385, https://doi.org/10.1016/j.jpowsour.2014.04.013.

[39] P. Ning, Q. Meng, P. Dong, J. Duan, M. Xu, Y. Lin, Y. Zhang, Recycling of cathode material from spent lithium ion batteries using an ultrasound-assisted DL-malic acid leaching system, Waste Manag. 103 (2020) 52–60, https://doi.org/10.1016/j.wasman.2019.12.002.

[40] S. Zhou, Y. Zhang, Q. Meng, P. Dong, Z. Fei, Q. Li, Recycling of LiCoO2 cathode material from spent lithium ion batteries by ultrasonic enhanced leaching and one-step regeneration, J. Environ. Manag. 277 (2021), https://doi.org/10.1016/j.jenvman.2020.111426.

[41] Y. He, X. Yuan, G. Zhang, H. Wang, T. Zhang, W. Xie, L. Li, A critical review of current technologies for the liberation of electrode materials from foils in the recycling process of spent lithium-ion batteries, Sci. Total Environ. 766 (2021) 142382, https://doi.org/10.1016/j.scitotenv.2020.142382.

[42] J. Liu, X. Bai, J. Hao, H. Wang, T. Zhang, X. Tang, S. Wang, Y. He, Efficient liberation of electrode materials in spent lithium-ion batteries using a cryogenic ball mill, J. Environ. Chem. Eng. 9 (2021) 106017, https://doi.org/10.1016/j.jece.2021.106017.

[43] T. Leißner, D. Hamann, L. Wuschke, H.-G. Jäckel, U.A. Peuker, High voltage fragmentation of composites from secondary raw materials – potential and limitations, Waste Manag. 74 (2018) 123–134, https://doi.org/10.1016/j.wasman.2017.12.031.

[44] R. Zhan, T. Payne, T. Leftwich, K. Perrine, L. Pan, De-agglomeration of cathode composites for direct recycling of Li-ion batteries, Waste Manag. 105 (2020) 39–48, https://doi.org/10.1016/j.wasman.2020.01.035.

[45] L. Wuschke, H.G. Jäckel, U.A. Peuker, Crushing of large Li-ion battery cells, Waste Manag. 85 (2019) 317–326, https://doi.org/10.1016/j.wasman.2018.12.042.

[46] C. Hanisch, W. Haselrieder, A. Kwade, Recovery of active materials from spent lithium-ion electrodes and electrode production rejects, in: Glocalized Solut. Sustain. Manuf. - Proc. 18th CIRP Int. Conf. Life Cycle Eng., Springer Science and Business Media, LLC, 2011: pp. 85–89. https://doi.org/10.1007/978–3-642–196 92-8_15.

[47] E. Fan, L. Li, X. Zhang, Y. Bian, Q. Xue, J. Wu, F. Wu, R. Chen, Selective recovery of Li and Fe from spent lithium-ion batteries by an environmentally friendly mechanochemical approach, ACS Sustain. Chem. Eng. 6 (2018) 11029–11035. ⟨https://pubs.acs.org/doi/10.1021/acssuschemeng.8b02503⟩.

[48] M. Wang, C. Zhang, F. Zhang, An environmental benign process for cobalt and lithium recovery from spent lithium-ion batteries by mechanochemical approach, Waste Manag. 51 (2016) 239–244, https://doi.org/10.1016/j.wasman.2016.03.006.

[49] L. Li, J. Ge, R. Chen, F. Wu, S. Chen, X. Zhang, Environmental friendly leaching reagent for cobalt and lithium recovery from spent lithium-ion batteries, Waste Manag. 30 (2010) 2615–2621, https://doi.org/10.1016/j.wasman.2010.08.008.

[50] D. Li, B. Zhang, X. Ou, J. Zhang, K. Meng, G. Ji, P. Li, J. Xu, Ammonia leaching mechanism and kinetics of LiCoO2 material from spent lithium-ion batteries, Chin. Chem. Lett. 32 (2021) 2333–2337, https://doi.org/10.1016/j.cclet.2020.11.074.

[51] X. Zhu, C. Chen, Q. Guo, M. Liu, Y. Zhang, Z. Sun, H. Song, Ultra-fast recovery of cathode materials from spent LiFePO4 lithium-ion batteries by novel electromagnetic separation technology, Waste Manag. 166 (2023) 70–77, https://doi.org/10.1016/j.wasman.2023.04.045.

[52] A.J. Da Costa, J.F. Matos, A.M. Bernardes, I.L. Müller, Beneficiation of cobalt, copper and aluminum from wasted lithium-ion batteries by mechanical processing, Int. J. Min. 145 (2015) 77–82, https://doi.org/10.1016/j.minpro.2015.06.015.

[53] H. Bi, H. Zhu, L. Zu, Y. Gao, S. Gao, Z. Wu, Eddy current separation for recovering aluminium and lithium-iron phosphate components of spent lithium-iron phosphate batteries, Waste Manag. Res. 37 (2019) 1217–1228. ⟨https://pubmed.ncbi.nlm.nih.gov/31486742/⟩.

[54] H. Bi, H. Zhu, L. Zu, S. He, Y. Gao, S. Gao, Pneumatic separation and recycling of anode and cathode materials from spent lithium iron phosphate batteries, Waste Manag. Res. 37 (2019) 374–385. ⟨https://pubmed.ncbi.nlm.nih.gov/30726173/⟩.

[55] X. Zhu, C. Zhang, P. Feng, X. Yang, X. Yang, A novel pulsated pneumatic separation with variable-diameter structure and its application in the recycling spent lithium-ion batteries, Waste Manag. 131 (2021) 20–30, https://doi.org/10.1016/j.wasman.2021.05.027.

[56] J. Sohn, S. Kim, D. Yang, H. Kim, K. Lee, Recycling of spent lithium-ion batteries used in electric vehicles by physical treatment and acid leaching, in: EARTH 2015 - Proc. 13th Int. Symp. East Asian Resour. Recycl. Technol., International Symposium on East Asian Resources Recycling Technology, 2015: pp. 807–811.

[57] A.M. Salces, I. Bremerstein, M. Rudolph, A. Vanderbruggen, Joint recovery of graphite and lithium metal oxides from spent lithium-ion batteries using froth flotation and investigation on process water re-use, Miner. Eng. 184 (2022) 107670, https://doi.org/10.1016/j.mineng.2022.107670.

[58] A. Vanderbruggen, N. Hayagan, K. Bachmann, A. Ferreira, D. Werner, D. Horn, U. Peuker, R. Serna-Guerrero, M. Rudolph, Lithium-ion battery recycling—influence of recycling processes on component liberation and flotation separation efficiency, ACS EST Eng. 2 (2022) 2130–2141. ⟨https://pubs.acs.org/doi/10.1021/acsestengg.2c00177⟩.